

Spectral Analysis of the Quantization of a Mixed System

Eoin Devane

January 8, 2011

Abstract

We investigate the quantization of a free particle interacting linearly with a harmonic oscillator. We extend the work of previous authors to obtain accurate and reliable estimates for the large energy levels in order to determine the spectral statistics of the system. We do this via an analytical study of the system in the two complementary regions of phase space, followed by attempts to undertake the requisite matching of the solutions numerically. We use matching conditions to obtain good approximations to a large number of eigenvalues, from which the statistics can be determined and compared with the long-standing conjectures as to their nature. This task has been started, but more work needs to be undertaken to complete the study.

1 Introduction

The field of quantum chaos — the investigation of features of the quantization of the systems that exhibit chaos in the classical regime — has developed greatly in recent decades [2], [6], [7]. To understand the quantum features that reflect classical chaos, one generally considers the behavior in the semiclassical limit. Strictly speaking, this is the limit as the effective value of Planck's constant tends to zero, a singular limit that is often difficult to study. However, in isolated systems, one can approach this limit by considering the asymptotic behavior of the energy levels as the energy becomes large [7]. The statistics of these high-energy levels can then be investigated. It is this approach that we take in this paper.

Among the most interesting systems to which to apply such methods are mixed regular-chaotic quantum systems, whose classical counterparts exhibit both integrable and chaotic behavior. One such system consists of a particle moving on a ring that is divided into two regions; at the boundaries between these two sections, the particle is pushed impulsively by an otherwise separately-evolving harmonic oscillator. This system has been shown to exhibit cleanly divided integrable and chaotic regions in classical phase space [1]. More recently, this system was quantized, and certain aspects

of the quantum version were studied [5]. The investigation in reference [5] focused on avoided crossings of energy levels and certain features of the Husimi distributions and their connections with the chaotic features of the classical system.

Reference [5] mentions the suitability of this system for a spectral study — determining and investigating statistical distributions based on the energy eigenvalues (eigenenergies) of the quantum system. In order to undertake this, we must obtain suitably accurate and reliable approximations to the eigenvalues of the system, particularly those at high energy values. The crucial quantities that must be analyzed are not the levels themselves, but the level spacings. This means that our approximations must be good enough to ensure that their ordered differences are close enough to their true values so that the spacings we obtain are reliably representative of the true spacings.

The rest of the paper is organized as follows. In section 2 we describe the quantum version of the system. We then proceed in section 3 to recap, and slightly correct, the method of reference [5] for the direct approximation of the levels. Following that, we present in section 4 our approach to the problem. In section 5 we test our method for one particular set of parameter values. We summarize our results in section 6 and discuss further work in section 7.

2 The Quantum System

The Hamiltonian describing the quantum system is, by means of the canonical quantization [5], given by

$$H = \frac{1}{2} \left(-\frac{\partial^2}{\partial x^2} - \frac{\partial^2}{\partial y^2} + y^2 \right) - \alpha \chi(x)y, \quad (1)$$

where x is the particle coordinate, which we restrict between -2 and L . The region $-2 < x < 0$ is the *interaction* region, for which $\chi(x) = 1$, and $0 < x < L$ is the *free* region, for which $\chi(x) = 0$. Additionally, y is the oscillator coordinate. We have chosen these particular domains for x and y , as opposed to the different ones used in the previous papers, for reasons of simplicity that will emerge later. The two non-dimensional parameters that determine the behavior of the system are α , representing the coupling strength, and L , representing the length of the free region.

3 Direct Approximation of the Levels

In a previous paper [5], Mainiero and Porter focused on calculating the low energy levels and then investigated the existence of avoided crossings between such levels. To do this, they formed a basis consisting of the eigenstates of the uncoupled ($\alpha = 0$) system. These eigenstates are denoted by

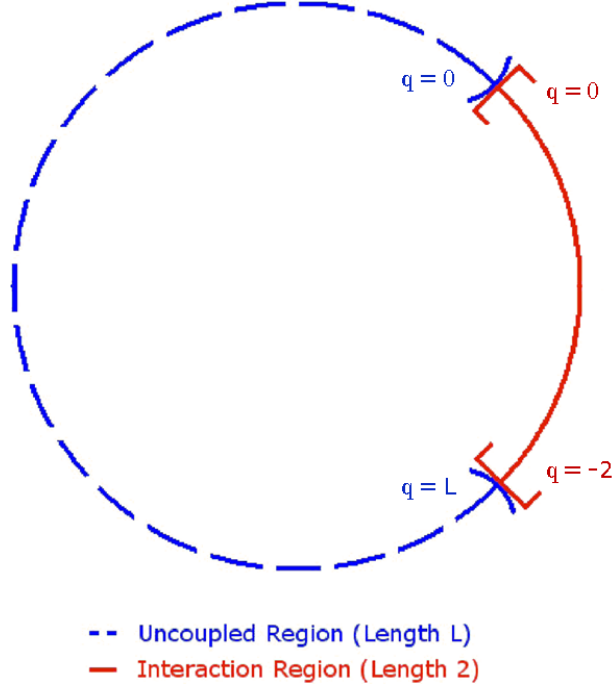


Figure 1: The configuration space corresponding to equation (1) (adapted from [5]).

$\psi_n^{\text{part}} \otimes \psi_k^{\text{osc}}$, where ψ_n^{part} and ψ_k^{osc} are, respectively, the n^{th} separable particle eigenstate and the k^{th} separable oscillator eigenstate, in the uncoupled regime. If one separates, solve, and introduces the operators

$$P_x = -i \frac{\partial}{\partial x}, P_y = -i \frac{\partial}{\partial y}, a^+ = \frac{1}{\sqrt{2}}(y + iP_y), a^- = \frac{1}{\sqrt{2}}(y - iP_y),$$

then one obtains the matrix expression

$$H = E_1 \otimes \mathbf{1} + \mathbf{1} \otimes E_2 - \alpha W_1 \otimes W_2, \quad (2)$$

where

$$(E_1)_{nn'} = \langle n | P_x^2 | n' \rangle = \frac{2\pi^2 n^2}{(2+L)^2} \delta_{nn'}, \quad (3)$$

$$(E_2)_{kk'} = \left\langle k \left| a^- a^+ + \frac{1}{2} \right| k' \right\rangle = \left(k + \frac{1}{2} \right) \delta_{kk'}, \quad (4)$$

$$(W_1)_{nn'} = \langle n | \chi(x) | n' \rangle = \begin{cases} \frac{i}{2\pi(n-n')} \left(1 - e^{\frac{4\pi(n-n')}{2+L}} \right) & \text{if } n \neq n' \\ \frac{2}{2+L} & \text{if } n = n' \end{cases}, \quad (5)$$

$$(W_2)_{kk'} = \frac{1}{\sqrt{2}} \left(\sqrt{k+1} \delta_{k,k'+1} + \sqrt{k'} \delta_{k,k'+1} \right). \quad (6)$$

The methods employed in the above calculations are exactly those from the reference [5]. However, it should be noted that the result we have obtained in equation (6) is a factor of 2 smaller than the result that was obtained there. This correction will change the numerical values of the results obtained in reference [5], but, as it simply amounts to an effective rescaling of the constant π , it will not change the physical nature or significance of the results obtained.

One is then able to calculate the low eigenvalues by applying the QR matrix factorization, as implemented in Matlab in the `eig` function, to a truncation of this Hamiltonian matrix. This method works particularly well and efficiently for calculating eigenvalues below certain bounds, defined by the computational power available, but becomes prohibitively expensive for larger ones. For example, on a modern mid-range laptop computer (2.00 GHz Intel Core2 Duo, 3GB RAM, Windows Vista Professional, Matlab R2010a), direct calculation reveals that the largest practical matrix truncation size is approximately 10000×10000 , and from this matrix one can reliably obtain all eigenvalues below 100. However, due to the nature of the algorithm applied, once one gets above 100, one starts to miss some eigenvalues.

4 A Matching Approach

Inspired by the work for the separable uncoupled case, we approach the general equation (1) by splitting the ring into the two natural regions (*free* and *interaction*). This gives two cases.

4.1 Case 1 - *Free*

We have $0 < x < L$ and

$$\frac{1}{2} \left(-\frac{\partial^2}{\partial x^2} - \frac{\partial^2}{\partial x^2} + y^2 \right) \psi = E\psi.$$

Now we separate $\psi = XY$, which, for a separation constant λ , gives

$$X'' + (2E - \lambda)X = 0, \tag{7}$$

$$-\frac{1}{2}Y'' + \frac{1}{2}y^2Y = \frac{1}{2}\lambda y^2Y. \tag{8}$$

Note that, with the requisite boundary condition that $\psi \rightarrow 0$ as $y \rightarrow 0$, (8) is the equation of a one-dimensional harmonic oscillator, so that we must have $\lambda = 2k + 1$, $k \in \mathbb{N}$. Therefore

$$X = A \cos \left(L\sqrt{2E - 2r - 1} \right) + B \sin \left(L\sqrt{2E - 2r - 1} \right),$$

$$Y = e^{-\frac{1}{2}y^2} H_k(y),$$

where H_k is the k^{th} Hermite polynomial.

Consequently, the general solution in the free region takes the form

$$\begin{aligned} \psi_{\text{free}} = \sum_{k=0}^{\infty} e^{-\frac{1}{2}y^2} H_k(y) & \left[A_k \cos \left(L\sqrt{2E - 2r - 1} \right) \right. \\ & \left. + B_k \sin \left(L\sqrt{2E - 2r - 1} \right) \right]. \end{aligned}$$

4.2 Case 2 - Interaction

The interaction region is defined as $-2 < x < 0$, and here equation (1) is

$$\frac{1}{2} \left(-\frac{\partial^2}{\partial x^2} - \frac{\partial^2}{\partial y^2} + y^2 \right) \psi - \alpha y \psi = E \psi.$$

Then proceeding in a manner exactly analogous to that employed in the free region, we obtain the general result for the wave function in the interaction region:

$$\begin{aligned} \psi_{\text{int}} = \sum_{l=0}^{\infty} e^{-\frac{1}{2}(y-\alpha)^2} H_l(y-\alpha) & \left[\bar{A}_l \cos \left(x\sqrt{\alpha^2 + 2E - 2l - 1} \right) \right. \\ & \left. + \bar{B}_l \sin \left(x\sqrt{\alpha^2 + 2E - 2l - 1} \right) \right]. \end{aligned}$$

It should be noted that we are using the overbar notation to denote new coefficients, different from those used in the *free* case, rather than complex conjugates.

4.3 Boundary Conditions

The first, and most obvious, boundary condition to employ is that of continuity across the boundaries. This yields

$$\psi_{\text{free}} \Big|_{x=0} = \psi_{\text{int}} \Big|_{x=0} \quad (9)$$

and

$$\psi_{\text{free}} \Big|_{x=L} = \psi_{\text{int}} \Big|_{x=-2}. \quad (10)$$

Equation (9), along with our expressions for ψ_{free} and ψ_{int} , then implies

$$\sum_{k=0}^{\infty} A_k e^{-\frac{1}{2}y^2} H_k(y) = \sum_{l=0}^{\infty} \bar{A}_l e^{-\frac{1}{2}(y-\alpha)^2} H_l(y-\alpha).$$

Now we use the orthogonality of the Hermite polynomials under their exponential weighting by integrating both sides against $H_n(y-\alpha)$ over the whole

y -axis. To do the right-hand integration, we assume that we can interchange the sum and the integral, and we use the relation

$$H_n(y - \alpha) = \sum_{r=0}^n \binom{n}{r} (-\alpha)^r H_{n-r}(y).$$

Then we can use orthogonality on both sides. Doing so and rearranging yields

$$\bar{A}_n = \sum_{r=0}^n A_r \frac{(-\alpha)^{n-r}}{(n-r)!}. \quad (11)$$

Analogously, but more difficult calculationally, working with (10) arrives at the second boundary condition

$$\begin{aligned} & \bar{A}_n \cos\left(2\sqrt{\alpha^2 + 2E - 2r - 1}\right) - \bar{B}_n \sin\left(2\sqrt{\alpha^2 + 2E - 2r - 1}\right) \\ &= \sum_{r=0}^n \frac{(-\alpha)^{n-r}}{(n-r)!} \left(A_r \cos\left(L\sqrt{2E - 2r - 1}\right) + B_r \sin\left(L\sqrt{2E - 2r - 1}\right) \right). \end{aligned} \quad (12)$$

We note that we require $|\alpha| < 1$ for convergence. This is simply a restriction imposed by our method; we would expect that the results obtained should still extend beyond this range, though a different method would need to be employed to verify this. Henceforth, we work with this restriction.

The fact that the jump in the energy, and consequently the momentum, is across boundaries specified entirely in the x -coordinate dictates that the momentum corresponding to the y -coordinate, P_y , should be continuous across each boundary. Consequently, we obtain the second set of boundary conditions from the relations

$$\left. \frac{\partial \psi_{\text{free}}}{\partial y} \right|_{x=0} = \left. \frac{\partial \psi_{\text{int}}}{\partial y} \right|_{x=0} \quad (13)$$

and

$$\left. \frac{\partial \psi_{\text{free}}}{\partial y} \right|_{x=L} = \left. \frac{\partial \psi_{\text{int}}}{\partial y} \right|_{x=-2}. \quad (14)$$

Differentiating these expressions and then applying the defining recurrence relation of the Hermite polynomials

$$H_{k+1}(y) = yH_k(y) - H'_k(y),$$

we see that the boundary conditions obtained from (13) and (14) are, respectively, exactly the relations (11) and (12).

Finally, we need a pair of boundary conditions pertaining to the x -momentum, $P_x = -i\frac{\partial}{\partial x}$. There is a jump in the energy across the boundaries

between the regions, so we expect that there will be a corresponding jump in P_x . Then, by symmetry, we have

$$\left. \frac{\partial \psi_{\text{free}}}{\partial x} \right|_{x=0} = \left. \frac{\partial \psi_{\text{int}}}{\partial x} \right|_{x=0} + Q \quad (15)$$

and

$$\left. \frac{\partial \psi_{\text{free}}}{\partial x} \right|_{x=L} = \left. \frac{\partial \psi_{\text{int}}}{\partial x} \right|_{x=-2} + Q. \quad (16)$$

Differentiating, and then integrating against $H_n(y - \alpha)$ in each case and expanding Q in the Hermite basis,

$$Q = \sum_{j=0}^{\infty} p_j e^{-\frac{1}{2}(y-\alpha)^2} H_j(y - \alpha),$$

the boundary conditions (15) and (16) become

$$\bar{B}_n = \sum_{r=0}^n \sqrt{\frac{2E - 2r - 1}{\alpha^2 + 2E - 2n - 1}} B_r \frac{(-\alpha)^{n-r}}{(n-r)!} - \frac{p_n}{\sqrt{\alpha^2 + 2E - 2n - 1}}. \quad (17)$$

and

$$\begin{aligned} & \bar{B}_n \cos\left(2\sqrt{\alpha^2 + 2E - 2r - 1}\right) + \bar{A}_n \sin\left(2\sqrt{\alpha^2 + 2E - 2r - 1}\right) \\ &= \sum_{r=0}^n \sqrt{\frac{2E - 2r - 1}{\alpha^2 + 2E - 2n - 1}} \frac{(-\alpha)^{n-r}}{(n-r)!} \left[B_r \cos\left(L\sqrt{2E - 2r - 1}\right) \right. \\ & \quad \left. - A_r \sin\left(L\sqrt{2E - 2r - 1}\right) \right] - \frac{p_n}{\sqrt{\alpha^2 + 2E - 2n - 1}}. \end{aligned} \quad (18)$$

We now have the four boundary conditions that we require — namely (11), (12), (17) and (18). We can substitute the results of the first two of these into the last two, to give the two crucial equations (for all $n \in \mathbb{N}$):

$$\begin{aligned} & \sum_{r=0}^n \frac{(-\alpha)^{n-r}}{(n-r)!} \left(A_r \left[\cos\left(L\sqrt{2E - 2r - 1}\right) - \cos\left(2\sqrt{\alpha^2 + 2E - 2r - 1}\right) \right] \right. \\ & \quad \left. + B_r \left[\sin\left(L\sqrt{2E - 2r - 1}\right) + \sqrt{\frac{2E - 2r - 1}{\alpha^2 + 2E - 2n - 1}} \sin\left(2\sqrt{\alpha^2 + 2E - 2r - 1}\right) \right] \right) \\ & \quad - \frac{p_n \sin\left(2\sqrt{\alpha^2 + 2E - 2r - 1}\right)}{\sqrt{\alpha^2 + 2E - 2n - 1}} = 0, \end{aligned} \quad (19)$$

$$\begin{aligned}
& \sum_{r=0}^n \frac{(-\alpha)^{n-r}}{(n-r)!} \left(B_r \sqrt{\frac{2E-2r-1}{\alpha^2+2E-2n-1}} \left[\cos \left(L\sqrt{2E-2r-1} \right) \right. \right. \\
& \quad \left. \left. - \cos \left(2\sqrt{\alpha^2+2E-2r-1} \right) \right] - A_r \left[\sin \left(2\sqrt{\alpha^2+2E-2r-1} \right) \right. \right. \\
& \quad \left. \left. + \sqrt{\frac{2E-2r-1}{\alpha^2+2E-2n-1}} \sin \left(L\sqrt{2E-2r-1} \right) \right] \right) \\
& \quad - \frac{p_n}{\sqrt{\alpha^2+2E-2n-1}} \left[1 - \cos \left(2\sqrt{\alpha^2+2E-2r-1} \right) \right] = 0.
\end{aligned} \tag{20}$$

We then require one further equation for each n . To obtain this, we note that the E are the eigenenergies, and the A_n and B_n are coefficients of the corresponding eigenvectors. However, if f is an eigenfunction corresponding to an eigenenergy λ , then so too is kf for all $k \in \mathbb{R}$. This implies that, for each fixed E , if we have a solution set A_n, B_n , then we should be able to multiply these coefficients by any real number and still have a solution set. This indicates that the p_n must depend linearly on the A_n, B_n . Assuming dependence on all of these, the simplest such relation is

$$p_n = q_n(A_n + B_n), \tag{21}$$

where the q_n are what will need to be determined. Due to its intuitive appeal, we work with this form for the p_n , though it remains an open problem to derive these expressions in a rigorous manner.

Substituting (21) into each of (19) and (20) and rearranging, we obtain a pair of equations for each $n \in \mathbb{N}$. Then we note that the $n = 0$ pair is homogeneous and linear in A_0, B_0 , so we have a dichotomy — either $A_0 = B_0 = 0$ or the determinant of the system is zero. This latter possibility gives an equation for E , and in turn determines a first set of possible eigenvalues. If the former is the possibility that holds, then we proceed to $n = 1$ and obtain an analogous dichotomy. We can work “up the ladder” of n in this way and thereby obtain a countable set of pairs of equations. For each n , the pair of equations must have zero determinant in order to have a non-trivial solution. Consequently, the sets of possible can be obtained from the following equations:

$$\begin{aligned}
& \left(\sqrt{\frac{2E - 2n - 1}{\alpha^2 + 2E - 2n - 1}} \cos \left(L\sqrt{2E - 2r - 1} \right) - \frac{q_n}{\sqrt{\alpha^2 + 2E - 2n - 1}} \right. \\
& \left. - \frac{\sqrt{2E - 2n - 1} - q_n}{\sqrt{\alpha^2 + 2E - 2n - 1}} \cos \left(2\sqrt{\alpha^2 + 2E - 2r - 1} \right) \right) \times \left(\cos \left(L\sqrt{2E - 2r - 1} \right) \right. \\
& \left. - \cos \left(2\sqrt{\alpha^2 + 2E - 2r - 1} \right) - \frac{q_n \sin \left(2\sqrt{\alpha^2 + 2E - 2r - 1} \right)}{\sqrt{\alpha^2 + 2E - 2n - 1}} \right) \\
& + \left(\sin \left(L\sqrt{2E - 2r - 1} \right) + \frac{\sqrt{2E - 2n - 1} - q_n}{\sqrt{\alpha^2 + 2E - 2n - 1}} \sin \left(2\sqrt{\alpha^2 + 2E - 2r - 1} \right) \right) \\
& \times \left(\sqrt{\frac{2E - 2r - 1}{\alpha^2 + 2E - 2n - 1}} \sin \left(L\sqrt{2E - 2r - 1} \right) + \sin \left(2\sqrt{\alpha^2 + 2E - 2r - 1} \right) \right) \\
& + \frac{q_n}{\sqrt{\alpha^2 + 2E - 2n - 1}} \left[1 - \cos \left(2\sqrt{\alpha^2 + 2E - 2r - 1} \right) \right] = 0.
\end{aligned} \tag{22}$$

We note that these equations generate the eigenenergies in countably many subsets — one for each equation — when given the values of the q_n . From the behavior of the approximations that we obtained earlier, we expect that the q_n should depend on the energy in some way and hence should not be viewed as constants in our equation. However, it is not obvious how to obtain the q_n analytically. Therefore, we adopt a numerical approach to determining these quantities.

4.4 The $\alpha = 0$ Case

In the uncoupled case, for which $\alpha = 0$, the system can be easily solved analytically by separation, so we can test (22) by comparison with these solutions. If $\alpha = 0$, then there is no jump in the oscillator equilibrium, so there should be no jump in the momenta, implying that $q = 0$. In this case, (22) simplifies to

$$\cos \left((L + 2) \sqrt{2E - 2n - 1} \right) = 1,$$

so

$$E = \frac{2k^2\pi^2}{(L + 2)^2} + \frac{1}{2} + n,$$

are the eigenenergies (exactly as can be shown to be given by the analytical solution).

4.5 The $q_n = 0$ Approximation

The numerical work detailed in later sections shows that the optimal values of the q_n are small, suggesting that we might gain a rough insight into the

behavior of the eigenvalues by considering the roots of the simpler equations for which all q_n are set to zero. Setting all $q_n = 0$, we note that the n^{th} equation becomes a function of $2E - 2n - 1$. Consequently, the n^{th} equation is just a translation of the $n = 0$ equation, so that if $\{E_i : i \in J\}$ are the roots of the 0^{th} equation (for some indexing set J), then the roots of the n^{th} equation are simply $\{E_i + n : i \in J\}$. Therefore, we have a *base* subset of eigenvalues corresponding to the $n = 0$ equation, and then a second subset equal to the *base* set incremented by one, a third subset equal to the *base* set incremented by two, and so on.

4.6 The General Case

Now we effectively consider $q_n \neq 0$ as a perturbation to the above $q_n = 0$ case. Consequently, we expect that the exact eigenvalues to come in a similar distribution to those above, namely one *base* subset (from the $n = 0$ equation) and then further subsets (from the $n = r$ case) that are approximately, but no longer exactly, equal to the *base* subset incremented by $r = 1, 2, 3, \dots$. We must remember that the q_n are not constants, but depend on the actual energy value.

There is an additional insight that one can gain from the simplifications above. Namely, in the $\alpha = 0$ case, the eigenvalues within each subset (i.e. corresponding to each value of n) are quadratically dependent on the other quantum number k , which determines the level number within the set. For sufficiently small α , we expect that this quadratic relationship should extend to the general case. Thus, we expect the levels within each subset in the general case to follow a roughly quadratic pattern, so an initial quadratic approximation of them might well be both reasonable and useful.

In short, we expect (though we have not shown this rigorously) to find the eigenvalues arranged in the form of a *base* subset coming from the $n = 0$ equation, which depend roughly quadratically on the level number within the subset, and then, for each $n \in \mathbb{N} \setminus \{0\}$, a further subset that is close to the *base* subset incremented by n . Though this argument provides some justification for the method we use, the main justification is really retrospective; the justification *is that it works!* Genuine justification remains an open problem; we expect that this may arrive by means of the dimensional analysis arguments hinted at in section 7.

4.7 Optimization of the q_n

Suppose that we fix the parameters α and L . Then we can use the method of Mainiero and Porter in [5] to obtain excellent approximations to the energy level at the lower end of the energy spectrum. We can use these approximations, together with the equation and our insights described above, to determine the optimal q_n — the values that forces equation (22) to output

the eigenvalues most accurately. Because each q_n has an energy (and hence a level number within the subset) dependence, we must optimize each q_n separately for each level number within the n^{th} subset. The numerical work suggests that, for each fixed pair (n, k) and any sufficiently accurate approximation of the eigenvalues, there is a unique $q_{n,k}$ such that the distance between the k^{th} root of equation (22) and the corresponding approximate eigenvalue is equal to zero. Thus, we are effectively finding the optimal $q_{n,k}$, each dependent on *two* quantum numbers. Consequently, the optimization can proceed as follows.

1. Generate the approximations to the small eigenvalues by the method of reference [5].
2. Enumerate these and manually select the first ten or so members of the 0^{th} subset.¹ For small α these can easily be spotted as the E for which there is an eigenvalue present in our enumerated list that is very close to $E + 1$ but there is none present very close to $E - 1$).
3. Find the quadratic curve of best fit through the scatter points of the above levels versus their level number (within the 0^{th} subset).
4. Use the quadratic equation to generate quadratic approximations to the 0^{th} subset energy levels. Order this list and call the ordered list R . Use the index k to label the elements of this list.²
5. Algorithmically search the list from step 1 to find the “true” level that is closest to each element of list R . Call this list S . This will give us a very good approximation of the small eigenvalues in the 0^{th} subset.
6. Find the root of equation (22) (for $n = 0$) that is closest to the k^{th} element of list S . Determine the value of q_0 that minimizes the distance between this root and the k^{th} element of list S . Call this $q_{0,k}$. Do this for all k .
7. Find the quadratic curve of best fit through the scatter points of all the levels obtained against their level number (within the 0^{th} subset). Call this list T .
8. For each n from 1 up to the square root of the matrix size (or somewhere lower), put $R = T + n$, and then repeat steps 5 and 6, but with n in place of 0 wherever it appears.

¹More gives better reliability - it is best to iterate somewhat, so use the first five to generate the next five, then those ten to give the next ten etc

²We do this because the r^{th} entry of R is our initial approximation to the r^{th} energy level within the 0^{th} subset of energy levels.

The aim of this method is to find relationships governing the $q_{n,k}$, so that we can determine an approximate analytical expression for the jump in the x -momentum, and thereby obtain accurate and reliable approximations to all the eigenenergies in a computationally efficient way.

Based on the process of obtaining the data that has been obtained (see the discussion in section 5), we observe that the method appears to work for a wide range of parameter values (as long as we maintain the technical restriction $\alpha < 1$). However, as one increases L , the distance between neighboring roots in each of equations (22) increases. Consequently, any implementation of this algorithm will have to use a larger number of sampling points, making it less efficient.

5 Test for Specific Parameter Values

We now consider the application of the above method by considering an example with parameter values $\alpha = 0.1$ and $L = 2$. The non-zero value of α and the sufficiently large L mean that, for values of E that are not too large, a significant portion of the classical phase space should be chaotic [1].

We proceed with the 8 steps listed above, starting with using the method of Mainiero and Porter [5] to generate the lower eigenenergies for use in the optimization. We use a matrix size of 10000 and look at values of n and k up to 90 for reliability. The results that we obtain show definite patterns both within each subset and across the different subsets.

5.1 Fixed n

To exhibit the behavior within each subset, we present the data from the 0th subset, which is representative of all those considered. In Figures 2 and 3, respectively, we plot the graphs of $q_{0,k}$ versus even k and versus odd k .

Figure 2 exhibits the clearest behavior, which is an apparently linear relationship. In fact, the Pearson product moment correlation coefficient of this data is 0.99999996085565. It should be noted that, for most of the k values, there turns out to be a range of $q_{0,k}$ for which the difference between our estimate and the element of the list of matrix eigenvalues (list A) is minimized to zero. Also, one should note that the aforementioned list A consists only of estimates (although they are extremely good ones). Hence, it seems plausible that this apparent linear relationship is truly reflective of a real linear relationship between $q_{0,k}$. Similar relationships appear to hold for the even k for all n .

For the case of odd k , however, the situation is somewhat more complicated. Figure 3 still shows a clear relationship between the two quantities, but it is no longer linear. Now we note the apparent asymptotic tendency towards a quantity close to 0.005. Indeed, the only quantity that would seem to make sense here from a dimensional perspective is $\frac{\alpha^2}{2} = 0.005$.

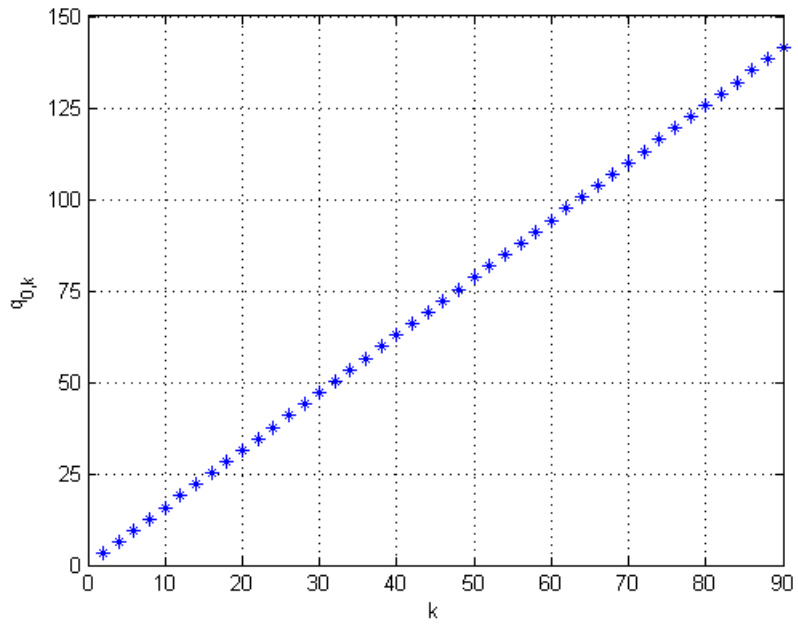


Figure 2: Plot of $q_{0,k}$ versus k for the even values of k below 90.

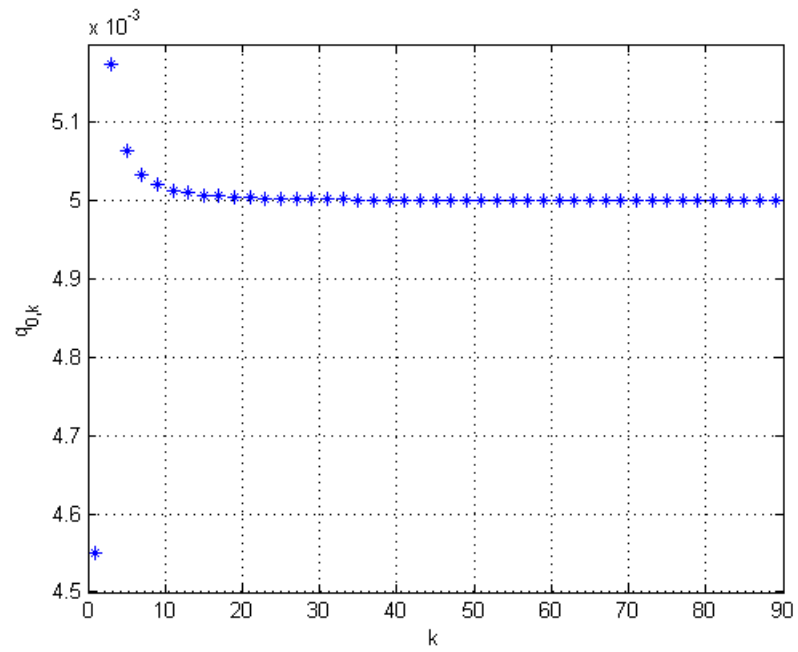


Figure 3: Plot of $q_{0,k}$ versus k for the odd values of k below 90.

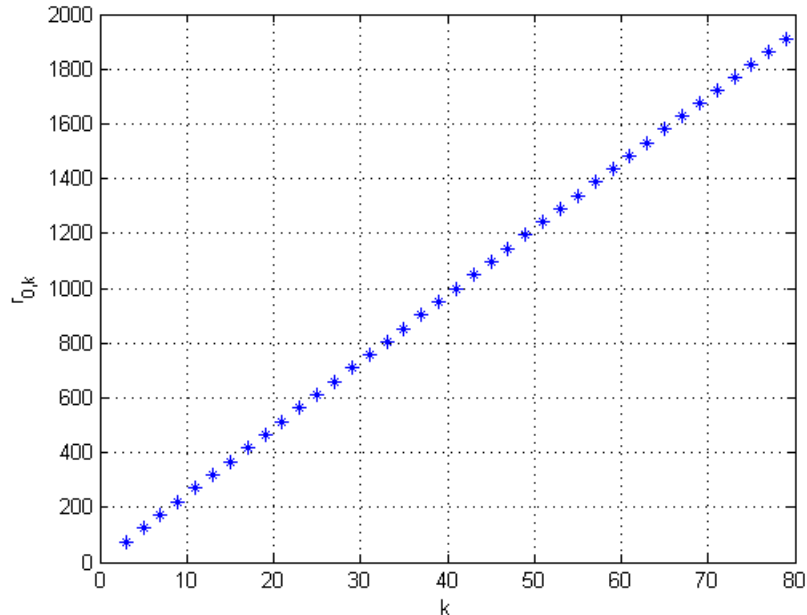


Figure 4: Plot of $r_{0,k}$ versus k for the odd values of k between 2 and 80.

Hence, guided by the shape of the data, we plot in Figure 4 the new quantity $r_{0,k} = \frac{1}{\sqrt{(q_{0,k}-0.005)}}$ versus odd k , between 2 and 80. We observe a good linear relationship, which suggests the asymptotic form

$$q_{0,k} = 0.005 + \frac{\Omega}{k^2}$$

for some constant Ω .

Due to the fact that we have obtained the results from these numerical simulations, this is one obvious place where dimensional methods could potentially be employed to verify that the power of 2 is in fact correct. Again, this argument generalizes to the case of non-zero n .

5.2 Fixed k

Now we consider the relationship with n . Let us begin with the simpler case of even k . In this case, for each fixed n , there is a linear relationship between $q_{n,k}$ and k . We represent this using the gradient and the y -intercept. We plot these quantities in Figures 5 and 6. These figures show excellent correlation, so we feel justified in extrapolating this relationship and thereby feel able to determine with accuracy the necessary values of $q_{n,k}$ for large ranges of n and k , provided that k is even.

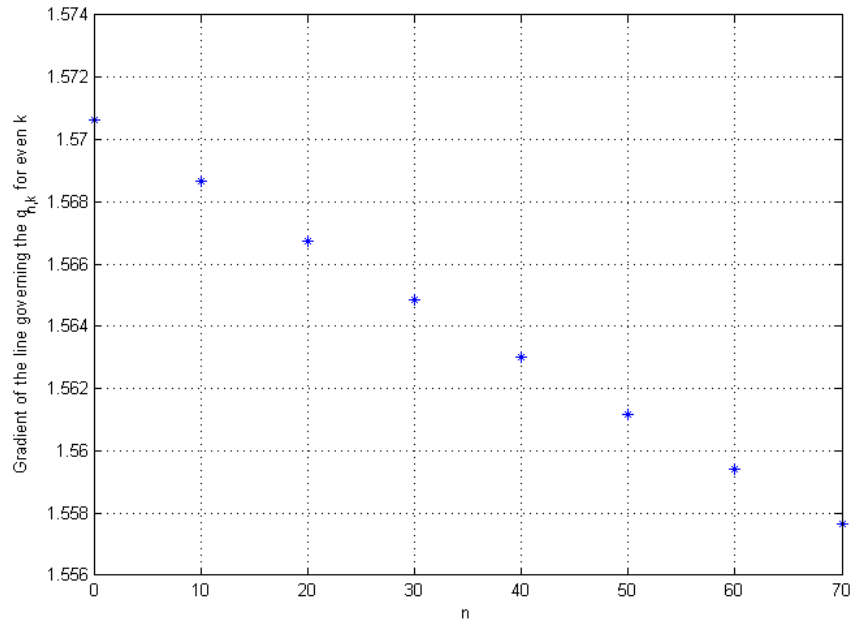


Figure 5: Plot of the gradient of the lines for $q_{n,k}$ versus n for even k .

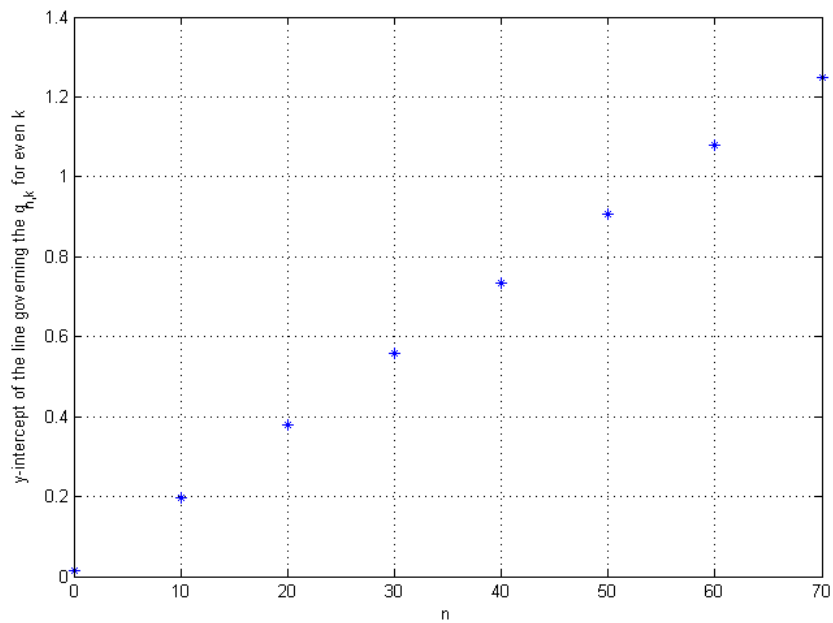


Figure 6: Plot of the y -intercept of the lines for $q_{n,k}$ versus n for even k .

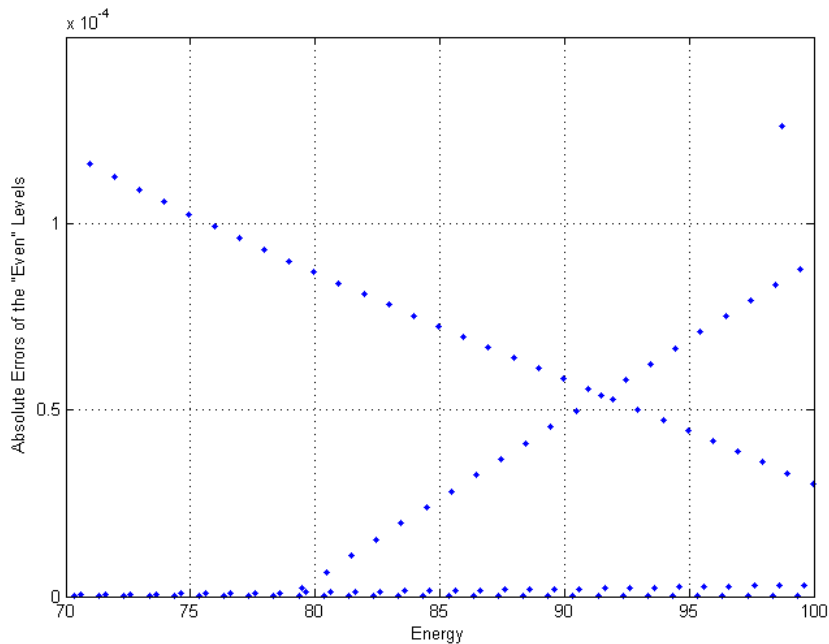


Figure 7: Absolute errors for eigenvalue estimates for even k .

The situation is less clear for the case of odd k . As mentioned previously, we can obtain a good expression governing the asymptotic behavior of the data we have for each n . However, the relationship linking these expressions, though apparently extant, is not clear, and is something that would be interesting to investigate in future work. For the work of the following section, we approximate Ω by means of exponential regression, though this is clearly not the true solution, as our expression is only really true in the limit of large energy. To find an equation valid across the whole energy scale, more work is needed.

5.3 Errors

We used only values of n below 70 for the matching, so that we would have some eigenenergies (between 70 and 100) left over from the matrix calculation to compare with our estimates. To do this, we determined our estimates as roots of Equation (22) using the relationships from the previous section to determine q_n . We then calculated the differences of our results from the relevant matrix eigenvalues. In Figures 7 and 8, we plot the results, separately for those from even k and odd k . We plot absolute, rather than relative, errors here, since the quantity that will eventually be of significance is the level spacing distribution [3], on which the absolute size of any errors will have an effect.

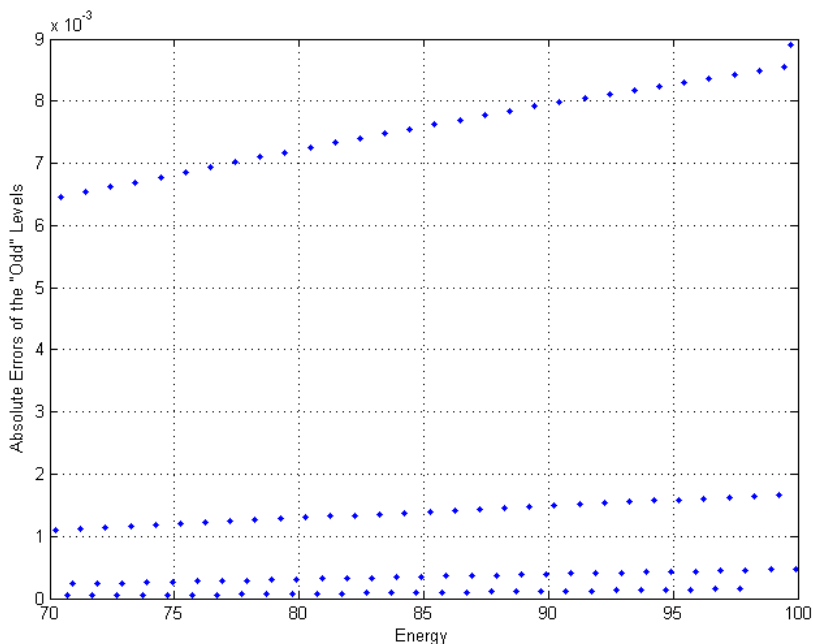


Figure 8: Absolute errors for eigenvalue estimates for odd k .

Note that the x -axes in Figures 7 and 8 both show energy from 70 up to 100, with the points plotted being fairly evenly distributed throughout this interval on each graph. This means that the larger absolute errors shown in Figure 8 compared with those in Figure 7 translate into larger relative errors.³ This allows us to conclude that, as expected, the agreement is much better for those from even k than for those from odd k , as more work is needed on elucidating the true relationship governing the $q_{n,k}$ in the odd case. Nonetheless, particularly in the even case, the agreement is excellent, and all of the errors appear to be systematic, rather than random, in nature. This strongly suggests that our approach, though somewhat painful numerically, is a promising one. It should be noted that we have actually performed such tests for five such sets. Further data can, and indeed should, be obtained by an analogous approach for different parameter values.

6 Conclusions

We have described what appears to be a promising approach to the problem of determining and analyzing the semiclassical level spacing distribution of the quantization of the particular classically chaotic system studied

³Comparing corresponding individual points from the two graphs makes this clear.

in [1]. By studying the quantum system analytically, we have derived equations (22) that can be used to determine the eigenenergies of the system. We have also formulated a method for doing this algorithmically. This algorithm gives a method that appears to work in the cases that we have studied, although its veracity has not been proved. We have already obtained five separate sets of data, of which the above is just one example. All of these have been analyzed as above, and each shows up such clear patterns as above. These patterns have been studied in a rough sense, though we expect that it should be possible to make this study more precise, by means of obtaining more data and considering the dimensions of the quantities present.

7 Further Work

As indicated above, all of the sets of data already obtained must be studied further. In addition, many further sets could easily be obtained and analyzed entirely analogously. Once sufficient data is obtained, the true relations governing the quantities q_n should be reasonably straightforward to obtain with the help of some dimensional analysis [4]. Further, it would be useful to obtain a rigorous mathematical derivation of equation (13) and the various heuristic assumptions that we used to infer it. In theory, it seems likely that this approach could give arbitrarily good estimates of the true eigenvalues; therefore, it ought to be an excellent method for obtaining the spectral statistics of the system.

8 Acknowledgments

This work was funded by an EPSRC Undergraduate Summer Research grant and undertaken under the supervision of Mason Porter. I would particularly like to thank him for all the advice, assistance and encouragement he provided. I would also like to thank Leonid Bunimovich for his most helpful suggestions at the very beginning of the project.

References

- [1] S. De Bièvre, P. E. Parris, and A. A. Silviu, *Physica D* **208**, 96 (2005).
- [2] M. C. Gutzwiller, *Chaos in Classical and Quantum Mechanics*, Springer (1990).
- [3] F. Haake, *Quantum Signatures of Chaos*, Springer (2001).
- [4] C. C. Lin and L. A. Segel, *Mathematics Applied to Deterministic Problems in the Natural Sciences*, SIAM (1988).
- [5] T. Mainiero and M. A. Porter, *Chaos* **17**, 043130 (2007).
- [6] M. A. Porter and R. L. Liboff, *American Scientist* **89**, 532-537 (2001).
- [7] H. J. Stöckmann, *Quantum Chaos: An Introduction*, Cambridge University Press (1999).